EXPERIMENTAL STUDIES IN STEREOLITHOGRAPHY RESOLUTION

Benay Sager, David W. Rosen, Meghan Shilling and Thomas R. Kurfess
The Woodruff School of Mechanical Engineering
Georgia Institute of Technology
Atlanta, GA 30332-0405

ABSTRACT

As we move towards micron-scale rapid manufacturing, it is critical to understand build resolution of Stereolithography technology. In order to determine the resolution limitations, positive and negative features on Stereolithography parts were built and analyzed. Results from several experiments were compared to an analytical model and important resolution issues are highlighted. Based on these experimental results, parameters that will maximize build resolution for a number of well-understood shapes are suggested in the paper. Build resolution experimental results, analysis, and measurement techniques are discussed. Conclusions are drawn related to feature shape as resolution limits are approached.

1. INTRODUCTION

Stereolithography (SLA) is a layered rapid prototyping process in which an UltraViolet (UV) laser is used to selectively cure a vat of liquid photopolymer resin in order to physically make a part from the generated CAD model. Even though the technology has been commercially available for over 15 years, no real attempt has been made to apply it to micro manufacturing until recently. With the interest in applying this technology to the micro manufacturing area comes the need to study the resolution of Stereolithography. More specifically, the limits of the resolution, both theoretical and empirical, need to be established.

It is important to make the distinction between resolution and accuracy before moving any further. Accuracy is defined as the measure of closeness to the nominal dimensions and geometry of the intended SLA part (Davis 2001). On the other hand, resolution refers to the fineness of the technology, quantifying the absolute limit of the technology.

2. STEREOLITHOGRAPHY RESOLUTION

Stereolithography resolution is affected by pre-build and build software (Software Imposed Parameters or SIP) and parameters that are inherent in the process (Process Parameters or PP). More information about the classification of resolution-affecting parameters could be found in (Sager and Rosen 2002). SLA resolution can be separated into horizontal (x-y plane) and vertical (z plane) resolution issues, and this paper will focus on the effect of horizontal resolution issues. The resolution limiting factors in horizontal domain are:

- Linewidth compensation (SIP)
- Laser beam spot diameter (PP)
- Stereolithography grid (PP)
- Resolution of the .stl file (SIP)

The laser beam spot diameter and the linewidth compensation parameter are the two parameters that have the most influence on horizontal resolution of the process on mesoscale manufacturing. Simply put, the laser beam spot diameter on the build surface is the smallest feasible feature size that can be scanned. Linewidth compensation determines how the laser beam should be offset when scanning a feature so that a cross-section would not be too small or too large. A brief description of these two parameters will be given. However, it is important to keep in mind that all four parameters would have significant influence when micron-size manufacturing is concerned.

2.1 Laser Beam Spot Diameter

The laser beam diameter is fixed at 200 μm on the build surface for most 3D Systems' SLA systems. In theory, this is the absolute limiting size of a feature that can be built. However, because of the scanning patterns, the smallest feature that can be built is around one-and-a-half times the laser beam diameter, around 300 μm. In high resolution systems such as the 3D Systems' Viper Si2 machine, the laser beam spot diameter is 75 ± 15 μm, and features as thin as 80 μm have been built using this spot size.

2.2 Linewidth Compensation

The linewidth compensation parameter ensures that the cross section of thin parts is scanned correctly by shifting over the center of the laser beam spot. In other words, linewidth compensation compensates for the width of the cured linewidth.

The default value for linewidth compensation is 125 μm, which is ½ of the laser beam diameter. When a rib that is 250 μm is to be built, if the default value of linewidth compensation is applied, the outline of the rib is shifted towards the inside of the profile and a line is created rather than a closed profile. Since a line is not interpreted by the SLA system as part of a cross-section, it would not be scanned. On the other hand, if a smaller linewidth compensation value such as 25 μm is used, the rib feature will be scanned. This would result in a thicker-than-desired rib that is 400 μm thick; however, the feature would not be altogether omitted. However, as aforementioned, it could also result in very inaccurate thin features.

3. ANALYTICAL BACKGROUND

Stereolithography is a complex process that is enabled by a number of mechanisms working together. Because of this, it is important to identify the main components that have a bearing on the theoretical resolution for the process.

As the laser beam is scanning along the vat surface, a cured line is formed. The shape of this line is a parabola (Jacobs 1992), and its cure depth is given as:

$$C_d = D_p \ln(E_{max} / E_c) \qquad \text{(Equation 1)}$$

where C_d is the cure depth, D_p is the penetration depth for a resin, E_{max} is the maximum centerline laser exposure on the build surface, and E_c is the critical exposure for a resin. Equation (1) is known as the working curve for SLA, where D_p and E_c are resin constants. In the horizontal platform, the width of the cured line depends on the laser beam spot radius as well as a resin constant:

$$L_w = W_o \sqrt{2C_d / D_p} \qquad \text{(Equation 2)}$$

where L_w is the cured linewidth and W_o is the laser beam spot radius. For the linear portion of the working curve, the range of values for the cure depth can be estimated as $D_p < C_d < 4D_p$, which is equivalent to the range $1 < C_d / D_p < 4$ (Jacobs 1992). Therefore, it is possible to speak of a meaningful range of theoretical cured linewidth values for the SLA process. This is shown in Table 1 for different SLA machines.

The width of a wall formed by a stack of scanned lines can be computed using Equation (3) (Rosen 2002), where n is the number of layers.

$$width = 2\left[\frac{W_o^2}{2}\ln\left(\sqrt{\frac{2}{\pi}}\,\frac{P_L}{W_o V_s E_c}\sum_{k=0}^{n-1}e^{-kt/D_p}\right)\right]^{\frac{1}{2}} \qquad \text{(Equation 3)}$$
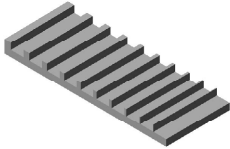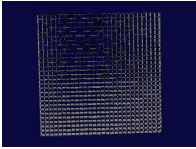
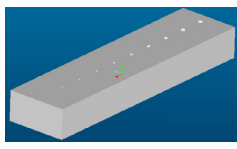Table 1. Typical Stereolithography cured linewidth values
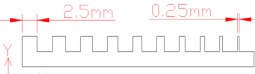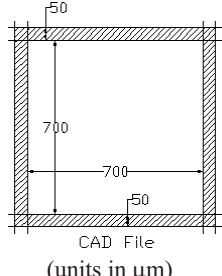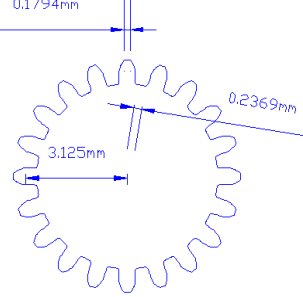
Machine		Resin		L_w (mm)			
Name	W_o (mm)	Name	D_p (mm)	Low	Typical		High
				$C_d/D_p=1$	$C_d/D_p=2$	$C_d/D_p=3$	$C_d/D_p=4$
SLA 250	0.12	DSM 7110	0.14	0.170	0.240	0.294	0.339
SLA 3500	0.125	SL 7510	0.145	0.177	0.250	0.306	0.354
Viper si2	0.125	SL 5510	0.12	0.177	0.250	0.306	0.354
Viper si2	0.125	DSM 10120	0.158	0.177	0.250	0.306	0.354
Viper si2 HR	0.0375	SL 5510	0.12	0.053	0.075	0.092	0.106
Viper si2 HR	0.0375	DSM 10120	0.158	0.053	0.075	0.092	0.106

From Table 1, it can be seen that the Viper si2 machine, when operated in the high-resolution mode, has a smaller laser beam spot radius. This means that thinner cured linewidth values of between 0.053 and 0.075 mm (53 to 75 microns) can be expected when using this machine. These values are important to keep in mind when the limits of resolution are considered.

4. EMPIRICAL STUDY

To quantify the effects of laser beam spot diameter and linewidth compensation on horizontal build resolution, a number of experiments were performed with different part cross-sections. Of particular interest was the predictability of negative and positive features. After building these cross-sections in Stereolithography machines, they were measured using a number of measurement techniques. The description of each cross-section, its outline, what it was intended to test, and how it was measured are shown in Table 2.

Table 2. Shapes used for empirical testing

Shape	Ribs	Grids	Gears	Holes
Outline				
Detail		CAD File (units in μm)		
What it is testing	Resolution for positive features	Resolution variation with build location	Resolution variation with curved surfaces/features	Resolution for negative features
How it is measured	Micrometer	White light Interferometer	Optical microscope	White light interferometer

The detail drawings show the horizontal cross-section for each shape as seen from the top view. The ribs were built using a number of different machine/resin combinations in order to quantify the resolution of different machines. The thickness of the ribs varied from 2.5 mm to 0.25 mm with 0.25 mm increments.

The rectangular grids were built in order to quantify how the thickness of a wall varies with respect to changing location on the build platform. The grids were built at the center of the vat and at the corners. The intended wall thickness for each grid was 50 μm.

A spur gear with 20 teeth was selected as a suitable profile for resolution study; not only because gears are very important in engineering, but also they have curved positive and negative profiles. The spur gear had 6.25 mm pitch diameter with an intended gap of 0.237 mm between teeth and tooth thickness of 0.179 mm.

In order to test the building ability of negative features, a part with holes was designed. This part had vertical holes that ranged from 1.25 mm to 0.125 mm in diameter with 0.125 mm increments. In all the parts built, the effect of the linewidth compensation parameter was also studied.

4.1 Data Collection and Analysis

Depending on the outline of the cross-section measured and the level of measurement detail required, different measurement techniques were used in this study. For measuring the thickness of the rib parts, using a micrometer was sufficient. For the gear cross-sections, the outline of the gears as well as the measurements were desirable. Therefore, an optical microscope with a 5x zooming lens was sufficient.

Interferometers, in particular white light interferometers, are currently being used to inspect mesoscale parts. Georgia Tech has a Zygo NewView 200 white light interferometer, which was used for collecting much of the grid and hole data. The interferometer uses the principle of interference to create a 3-dimensional surface profile of the parts. This data, however, is limited to a single view due to the slope limitations on measurement. Because the white light interferometer was initially created to measure surface characteristics such as surface roughness, it was designed to have very good resolution in the z-direction (out of plane). This resolution is more than adequate for mesoscale parts. The resolution in the lateral (x and y) directions, however, is not quite as good but will be sufficient for initial measurements. The lateral resolution is dependent on the objective being used. For the objectives in the Precision Machining Laboratory the lateral resolutions are 2.2 μm and 8.8 μm (for the 10x and 2.5x objectives, respectively) at regular camera resolution.

Conventional coordinate metrology is not appropriate for the type of data that are gathered using a white light interferometer. A single surface does not hold enough information for comparison to a CAD model or to an analytic surface (other than a plane). Because a CAD model is a series of surfaces that intersect, data from other surfaces are needed to properly orient the model or surface to the data. Due to this limitation, two-dimensional curves such as lines and circles are of interest.

For two-dimensional analysis, the data on a single surface are not what need to be analyzed. The edges of the data hold the important information. Therefore, it is necessary to extract edge data points from the original point cloud before any dimensional analysis can be performed. The edge point extraction takes several steps. First, a plane is fit to the surface data and an "image" is created. The pixel size of the image is set to the distance between the evenly spaced data points and the intensity, or color, of the pixel is directly related to the height of the pixel above the fit plane. After the "image" is created, a median filter is applied to remove noise.

After being filtered, edge points are either located by binarization and a simple row and column sweeping algorithm or an edge detector and contour tracking algorithm based on the idea of finding the center of mass in combination with a contour tracking technique. The edge points can then be analyzed by being fit to two-dimensional shapes such as lines, circles, and ellipses. This entire process is illustrated in Figure 1.
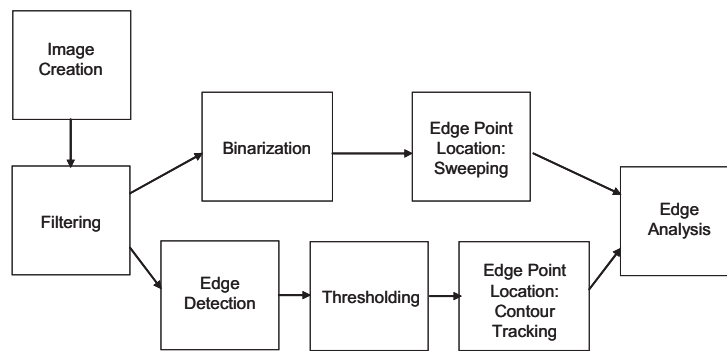
Figure 1: Analysis Flowchart

The methods described above have been validated using generated test data of circles and bars. Perfect circles and perfect bars yielded perfect results. When known noise was added, both sets yielded expected results. This procedure is fully outlined in (Shilling 2003).

4.2 Rib Parts
The outline of the rib parts and their detail cross-section were presented in Table 2. The rib parts were built using a number of machine/resin combinations, linewidth compensation, and layer thickness values, which are shown in Table 3. The goal was to quantify the resolution for each machine, along with the effect of different linewidth compensation values. In short, four comparative studies were done with the rib parts:

1. Thickness at tip of rib versus thickness at base of rib
2. Thickness of rib on top surface of build versus thickness of rib on bottom surface of build
3. Resolution of Stereolithography machine used
4. Resolution with respect to linewidth compensation value used

The thickness values at the tip of ribs were very similar to those at the base of ribs. It should be kept in mind that the distance between the tip and base of each rib is very short, about 2.5 mm. Therefore, such a small change in location of the laser beam as it was scanning the parts would not cause a significant change in the resolution of the final parts.

It is known that upfacing and downfacing surfaces in SLA have different resolution. This is partly due to the curing effects, and partly due to the fact that at the bottom of each build support

structures are anchored to the build platform (Jacobs 1996). For all six rib parts built, the thickness for a particular rib (rib 5) at the top and bottom surfaces is shown in Figure 2. There is a consistent thickness difference between bottom and top surfaces. This thickness difference is quantified in Table 4.

Table 3. Build parameters for rib parts 1-6

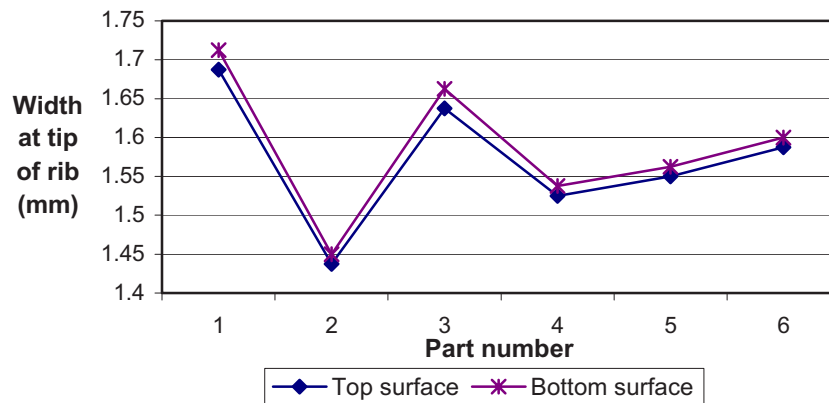| Part	Machine	Resin	Linewidth Comp. (mm)	Layer Thickness (mm)
1	SLA 3500	SL 7510	0.125	0.004
2	SLA 250	DSM 7110	0.125	0.004
3	SLA 250	DSM 7110	0.025	0.004
4	Viper Si2	SL 5510	0.0375	0.002
5	Viper Si2	SL 5510	0.01875	0.002
6	Viper Si2	SL 5510	Off	0.002

Figure 2. Top versus bottom surface for rib 5 width

Table 4. Difference in thickness between top and bottom surfaces for rib 5

Part number	Bottom surface thickness for rib part number (mm)	Top surface thickness for rib part number (mm)	Difference (μm) [Bottom – Top]
1	1.7125	1.6875	25
2	1.45	1.4375	12.5
3	1.6625	1.6375	25
4	1.5375	1.525	12.5
5	1.5625	1.55	12.5
6	1.6	1.5875	12.5

In Table 4, it can be seen that the thickness difference varies between 12.5 and 25 microns. This is an expected result, since the bottom surface of SLA builds typically have poorer resolution. When a SLA layer is scanned, in order to make sure it would anchor to the previous layer, it is "overcured" by a specified thickness into the previous layer. Additional overcuring of a number of layers causes the bottom surface of a SLA build to have thicker cross-sections than intended; hence a poorer resolution than top build surface. Therefore, it can be concluded that the top surface has features that are on average between 10-20 microns thinner than the bottom surface.

Another aspect of this study is quantifying the resolution of different SLA machines used. For each rib, the difference between the intended and measured thickness for different machines

is shown in Figure 3. It can be seen that when the default value for the SLA 250 machine was used, a part whose ribs were thinner than intended was obtained. On the other hand, as expected, the Viper si2 machine high-resolution build style produced parts with highest resolution.
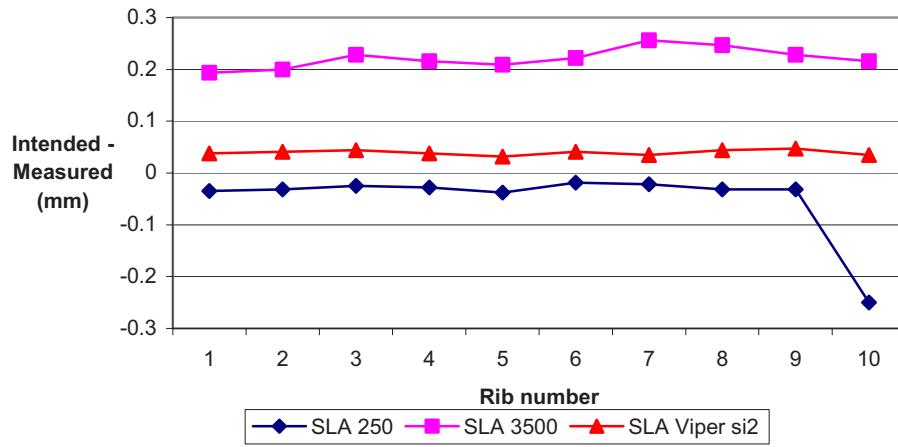

Figure 3. Average dimensional error for different SLA machines

A comparison of rib width values based on the different linewidth compensation values that can be used when preparing a build for the Viper si2 machine was made. Three different linewidth compensation values were used: the default value of 0.0375 mm, 0.01875 mm, and 0 mm. These different values and their resulting measurements are shown in Table 5.

Table 5. Comparison between expected and measured error

Linewidth compensation value used (μm)	Analytical expected error (μm)	Average measured error (μm)	Error discrepancy (μm)
37.5	0	39	**39**
18.75	37.5	57	**20**
0	75	104	**29**

As shown in Table 5, the lowest average error of 39 microns was obtained when the default linewidth compensation value of 37.5 microns was used. When the same default linewidth compensation value is used, the expected error is zero because the thickness of the laser beam is adequately compensated for. There seems to be a consistent error between the measurements and expected results when different linewidth compensation parameter values are used. It can be argued that by accounting for the error based on linewidth compensation value used, the error between the intended and measured thickness could be reduced. Table 5 presents expected error discrepancy within the range of 20-40 microns based on empirical results. It is clear that the parts built will be thicker than intended, and this value can be quantified as between 20 and 40 μm.

4.3 Grid Parts
The grid parts were built for a number of studies, including build location, orientation, and effect of linewidth compensation parameter on build resolution (Sager 2003). However, in this paper, only the effect of build location on build resolution will be presented. Four identical test parts were built simultaneously at the four corners of the build platform of the Viper si2 machine. The labeling for the locations of these parts is presented in Figure 4. Each grid part had

the dimensions of 25 mm by 25 mm in x and y directions respectively. The distance between the center of the vat and the center of the grid parts was 112.5 mm.
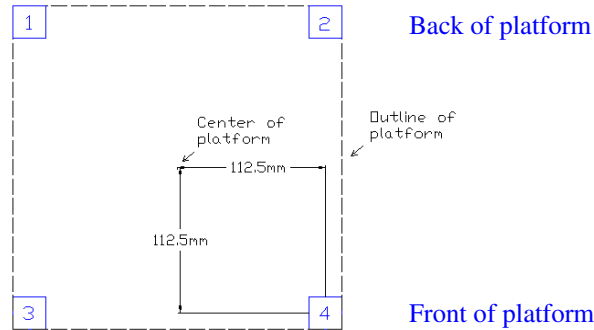

Figure 4. Location of grid parts on build platform

Measurements of the vertical cross-section of the parts taken by researchers at Siemens AG yielded results that suggest a heavy dependence of wall thickness on build location, as shown in Table 6. These measurements were taken from the grids around the center of each grid part and represent the average thickness of the walls. For each wall, the thickness was measured at three locations. These locations were towards the top of the wall, around the center of the wall, and towards the bottom of the wall.

Table 6. Grid average wall thickness with respect to build platform location

Position on platform	Thickness at location (μm)			Representative thickness (μm)
	1	2	3	
Center	126	133	121	127
1	226	265	253	248
2	210	246	274	243
3	250	263	275	263
4	171	217	184	191

Ignoring the smallest and largest values that were obtained at corners 4 and 3 respectively, the representative thickness at the corners can be taken as 243-248 μm. When compared to the wall thickness at the center of the build platform of 127 μm, this value is almost doubled. Such a difference between wall thickness values at center and corner of the build platform suggests that location on the build platform plays a major role in determining how thick a wall will become. This could be attributed to the change in laser beam characteristics as the laser beam moves away from the center of the build platform. For example, in order to adequately calculate the shape of cured line, the changes in the shape and size of the laser beam radius must be taken into account. Moreover, as we move away from the center of the build platform, the laser beam becomes out of focus, causing the wall thickness to become larger.

In addition to change in wall thickness with respect to build location, change in wall thickness with respect to vertical location was observed. This phenomenon is a direct result of overcuring each layer and is shown in Figure 5. In Figure 5, the bottom of the wall is the right side. As shown, the thickness at the bottom of the wall is around 130-145 μm. The left side of Figure 5, which corresponds to the top of the grid wall, was measured to be around 100 μm under the microscope.
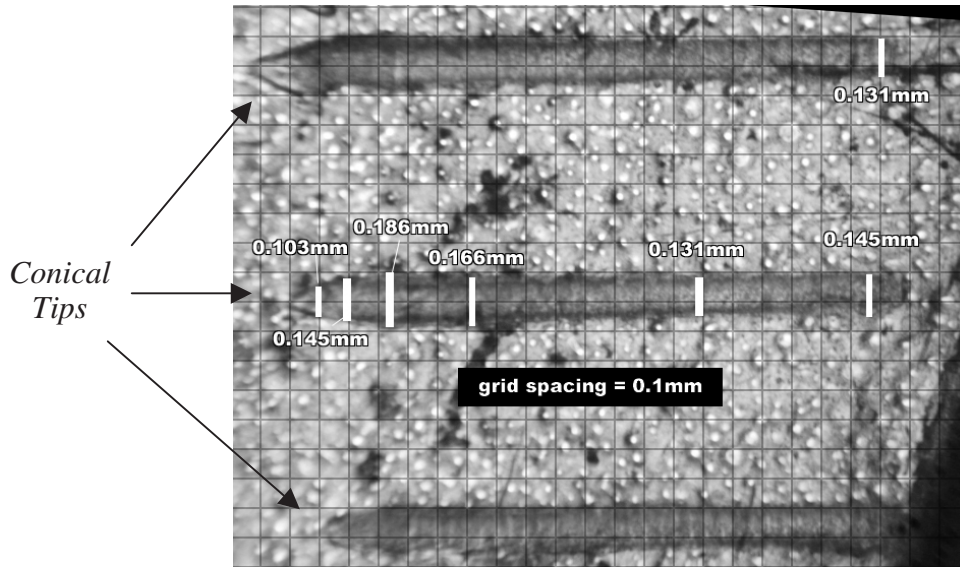
77

Figure 5. Vertical cross-section of grid walls

As aforementioned, the walls are thinner at the top due to the lack of overcure and print through for the latest-built layers. Print-through is a Stereolithography error that accumulates on a lower layer when an upper layer is scanned. The analytical model expressed by Equation (3) enables an explanation of this cone-tip effect (Rosen 2002; Sager 2003). This model suggests that the wall thickness of the build surface is 78 µm and the representative wall thickness is 95 µm (Sager 2003) for the Viper si2 high-resolution build style. This 17 µm discrepancy is in the middle of the measured overcure related error range of 10 - 25 µm. A representative wall thickness can be computed by adding the analytical thickness estimate to the linewidth compensation error range (20 - 40 µm). This yields an expected wall thickness range of 115 - 135 µm, which is smaller than the observed thicknesses. Additional research is needed to investigate this difference.

Table 7. Analytical, empirical, and expected empirical values for grid part walls

Measurement	Wall thickness on build surface (µm)	Representative wall thickness (µm)
Analytical	78	95
Empirical	100	130~145
Expected range	78 + (20~40) = **98~118**	95 + (20~40) = **115~135**

4.4 Holes

A hole study was performed to determine both the resolution of negative features as well as the changes in hole diameter from the top surface of the part to several layers into the part. In addition to comparing feature sizes in the top and lower layers, the purpose of this test was to determine the smallest hole that could be built.

After initial measurement, the part was ground using a small sample grinder to get a surface finish sufficient for measurement by the interferometer, so that the size of holes beneath the top surface can also be measured. From visual inspection, this was determined to be the 0.375 mm-diameter hole. After x-y-z data sets were collected using the interferometer, the data was

analyzed according to the steps outlined earlier in this paper. The results from measurement of the holes, as well as expected results are presented in Table 8.

Table 8. Radii from Hole Test Parts (in μm)

Circle	PART LOCATION		
	Expected (1)	Center (2)	Center ground (3)
A (1)	635.00	559.67	614.19
B (2)	571.50	500.80	623.16
C (3)	508.00	569.12	496.11
D (4)	444.50	462.41	446.43
E (5)	381.00	386.75	384.09
F (6)	317.50	319.17	312.55
G (7)	254.00	251.93	247.38
H (8)	190.50	193.63	190.50
I (9)	127.00	122.59	110.56
J (10)	63.50	46.09	-

The parts were measured using the Zygo New View 200 white light interferometer with the 10X objective (2.2.μm lateral resolution). There were problems with the Zygo stage, so the largest area that could be analyzed was approximately 700 by 500 μm. This caused some problems with the circles of larger diameters, but was sufficient for circles of smaller diameters.

Not enough data from the largest three holes in the hole test parts was collected to allow for reliable measurement. Although the results are presented, the values given might not represent the actual values of the radii of the holes. Additionally, the smallest hole was not present after the specimen was ground. The difference between the intended and measured hole radii is presented in Figure 6.
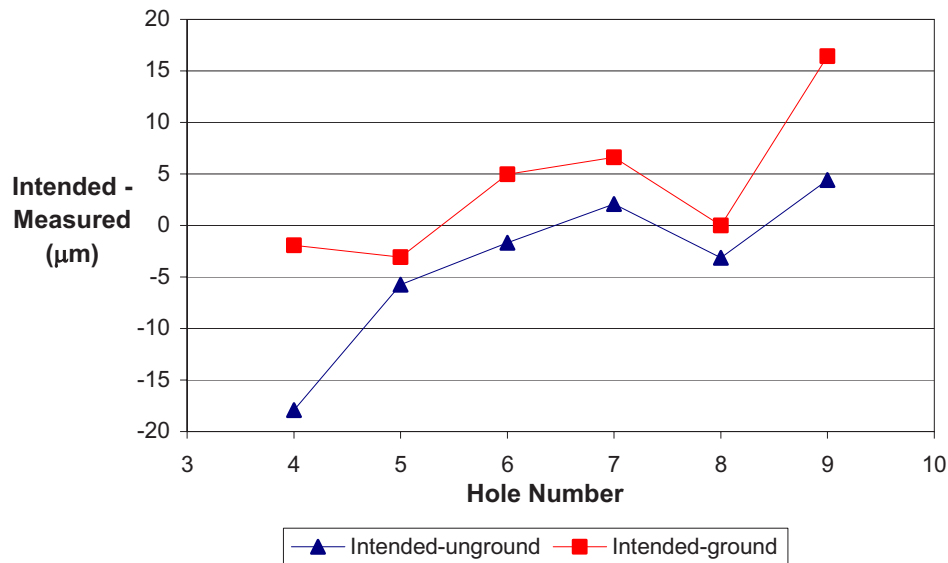

Figure 6: Comparison of ground and unground part

The results from comparing the ground part to the same unground part are presented in Figure 6, ignoring the largest three holes because of problems with the interferometer and the smallest hole because of its disappearance. It is seen that the diameters of the holes for the ground part are slightly smaller than that of the unground part in all cases, reflected by the larger difference between intended and measured hole diameters. This is consistent with the idea that the lower layers are exposed to more UV light; thus have a chance to cure more thoroughly.

4.5 Gears

A number of 6.25 mm-diameter spur gears were built in order to study resolution of curved cross-sections. The gear had teeth width of 179 μm and gap between teeth of 237 μm. The average thickness of gear teeth was 186 μm on top and 198 μm on bottom surface when small feature compensation parameter (SFP) was used. The gap between gear teeth, a negative feature, was 312 μm on top and 280 μm on bottom surface when SFP was used.

It can be said that SFP enabled generation of thin positive features that are more dimensionally accurate on the top surface of a build. In addition, the profile of the gear teeth was much sharper with the use of SFP. It was noticed on the SLA parts that some of the gear teeth lost their curved involute profile accuracy because they were too thin, which shows the limits of SLA resolution were reached with this spur gear profile.

5. CONCLUSIONS AND FUTURE WORK

With the rib parts built, it can be concluded that the bottom surface of SLA parts are thicker than the top surface. For the SLA Viper si2 system, the thickness discrepancy has been measured to be 20-40 μm, which is consistent with the analytical model of the curing process. The grid part experiments suggest that as we move away from the center of build platform, the resolution of SLA machines changes dramatically. Based on the empirical results and comparison with analytical models, a range of expected thickness values can be specified for high aspect ratio walls. Even though the Viper si2 system has a laser beam spot diameter of 75 μm, the realistic range for representative wall thickness is 115-135 μm. The ability to build small negative features using SLA technology has been demonstrated. However, more work is needed in quantifying the smallest negative feature that can be built. For certain shapes that are well understood, values for certain software parameters that would maximize build resolution are presented in Table 9.

Table 9. Use of build parameter values to obtain maximum build resolution

Build/ Recoat Parameter	Geometry / Part			
	Grids/ Thin walls and/or features	*Ribs*	*Gears*	*Lenses/ curved surfaces*
Linewidth compensation	Off	Default	Default	Default
Small feature preservation compensation (*Viper si2 only*)	On			
High resolution spatial tolerance (*Viper si2 only*)	On if highly tessellated area			On
Stl file deviation	Lowest allowable surface deviation			$\delta = C_{res} * R$, C_{res}=3.4E-05
Build orientation	45-degree	Vertical	Normal	Vertical
Build location	Center of build platform			
Sweeping	On			

The linewidth compensation parameter's default value should be used for builds other than thin walls. For parts that have thin walls or small features, turning the linewidth compensation off will ensure that the small feature is not omitted by the laser. This is critical for all the SLA machines that do not have small feature preservation compensation parameter.

The laser beam spot diameter is the biggest contributor to the limitation of SLA resolution. The spot diameter determines the size of the smallest feature that could be built on the horizontal platform. Since SLA is a stacking of a number of two-dimensional layers, it can be said that the resolution in the horizontal direction dictates the resolution in the vertical direction. Therefore, being able to control the laser beam spot diameter would improve the process resolution greatly.

For maximum x-y resolution, parts should be built in the center of the build platform if possible. In addition, using the sweeper blade ensures that the resin on the top surface of the SLA build is evenly distributed after each layer is scanned. Ribs or any other high aspect ratio features should be built in the vertical orientation to reduce stair steps.

Although white light interferometry was originally developed for surface measurements, it can be a useful tool in mesoscale part characterization when combined with several image-processing techniques. This method, however, is quite limited in its lateral resolution, speed, and three-dimensional measuring capabilities. In order to increase the speed and completeness of the measurement, new systems need to be developed.

In order to truly quantify the resolution of SLA technology, a study of three-dimensional resolution is needed. In the future, more experiments should be performed with negative features, including shapes that are rectangular such as a square-shaped hole. In addition, a comprehensive cure model that will take into account the effect of focus depth, change of laser beam angle, and resin properties is under study.

ACKNOWLEDGEMENTS

REFERENCES

Davis, B. E. 2001. "Characterization and Calibration of Stereolithography Products and Processes", *Master's Thesis*, Georgia Institute of Technology, Atlanta, GA.

Jacobs, P. F. (1992). Rapid Prototyping & Manufacturing: Fundamentals of Stereolithography, Society of Manufacturing Engineers.

Jacobs, P. F. (1996). Stereolithography and other RP&M Technologies: from Rapid Prototyping to Rapid Tooling, Society of Manufacturing Engineers.

Rosen, D. W. (2002). ME 7227 Rapid Prototyping in Engineering Class Notes. Atlanta, GA, Georgia Institute of Technology.

Sager, B. 2003. "A Method for Understanding and Predicting Stereolithography Resolution", *Master's Thesis*, Georgia Institute of Technology, Atlanta, GA.

Sager, B. and D. Rosen (2002). Stereolithography Process Resolution. Solid Freeform Fabrication Symposium, Austin, TX.

Shilling, K. M. 2003. "Two Dimensional Analysis of Mesoscale Parts Using Image Processing Techniques", *Master's Thesis*, Georgia Institute of Technology, Atlanta, GA.

Vantico Incorporated (2002). Vantico web page: http://www.vantico.com.